Strongly Coupled Data Assimilation Using Leading Averaged Coupled Covariance (LACC). Part I: Simple Model Study*

FEIYU LU

Nelson Institute Center for Climatic Research, and the Department of Atmospheric and Oceanic Sciences, University of Wisconsin–Madison, Madison, Wisconsin

ZHENGYU LIU

Nelson Institute Center for Climatic Research, and the Department of Atmospheric and Oceanic Sciences, University of Wisconsin–Madison, Madison, Wisconsin, and Laboratory for Climate, Ocean and Atmosphere Studies, Peking University, Beijing, China

SHAOQING ZHANG

NOAA/Geophysical Fluid Dynamics Laboratory, Princeton, New Jersey

YUN LIU

Nelson Institute Center for Climatic Research, and the Department of Atmospheric and Oceanic Sciences, University of Wisconsin–Madison, Madison, Wisconsin

(Manuscript received 25 September 2014, in final form 29 April 2015)

ABSTRACT

This paper studies a new leading averaged coupled covariance (LACC) method for the strongly coupled data assimilation (SCDA). The SCDA not only uses the coupled model to generate the forecast and assimilate observations into multiple model components like the weakly coupled version (WCDA), but also applies a cross update using the coupled covariance between variables from different model components. The cross update could potentially improve the balance and quality of the analysis, but its implementation has remained a great challenge in practice because of different time scales between model components. In a typical extratropical coupled system, the ocean–atmosphere correlation shows a strong asymmetry with the maximum correlation occurring when the atmosphere leads the ocean by about the decorrelation time of the atmosphere. The LACC method utilizes such asymmetric structure by using the leading forecasts and observations of the fast atmospheric variable for cross update, therefore, increasing the coupled correlation and enhancing the signal-to-noise ratio in calculating the coupled covariance. Here it is applied to a simple coupled model with the ensemble Kalman filter (EnKF). With the LACC method, the SCDA reduces the analysis error of the oceanic variable by over 20% compared to the WCDA and 10% compared to the SCDA using simultaneous coupled covariance. The advantage of the LACC method is more notable when the system contains larger errors, such as in the cases with smaller ensemble size, bigger time-scale difference, or model biases.

1. Introduction

Coupled data assimilation (CDA) shows great promise as a capable and comprehensive method for generating

---

climate analysis and providing initial conditions for climate prediction (Zhang et al. 2007; Sugiura et al. 2008; Saha et al. 2010; Dee et al. 2011). In CDA systems, observations are assimilated into one or more model components, and information is exchanged between different components dynamically and statistically. Zhang et al. (2007) developed the first CDA system in a fully coupled general circulation model, the Geophysical Fluid Dynamics Laboratory's Coupled Model, version 2 (CM2). The National Centers for Environmental Prediction

(NCEP) also started using coupled models to generate first-guess forecasts for their Climate Forecast System Reanalysis (CFSR; Saha et al. 2010). Compared with traditional single-component data assimilation (DA) systems, CDA is expected to produce self-consistent state estimates as well as optimal initialization for coupled model predictions (Zhang et al. 2007; Sugiura et al. 2008; Singleton 2011).

There are two levels of coupling in regards to the exchange of information in the analysis stage (Liu et al. 2013; Han et al. 2013). In the weakly coupled data assimilation (WCDA), the analysis increments are calculated and applied separately in each model component such that the coupling between different components is accomplished only dynamically through cross-component fluxes in the forecast stage. Atmosphere data assimilation (ADA) and ocean data assimilation (ODA) are the two most common components of a WCDA system. In contrast, the strongly coupled data assimilation (SCDA) applies the analysis increments using the fully coupled error covariance, especially the coupled covariance between variables from different model components (hereafter ''cross covariance'' and ''cross correlation,'' respectively). As a result, the coupling between different components is accomplished not only dynamically in the forecast stage, but also statistically through the coupled covariance in the analysis stage. In an SCDA system, the observed information in one model component can be directly projected onto another, resulting in instantaneous adjustment and balanced analysis increments. In this paper, the update process between model components will be called ''cross update.'' The WCDA has been adopted in previous researches (Zhang et al. 2007; Sugiura et al. 2008; Saha et al. 2010), however, the study of the SCDA has remained in the exploration stage.

In principle, the use of cross covariance should add additional information and improve the analysis. This has been recognized, for example, in a simple coupled model study (Liu et al. 2013). However, the implementation of the SCDA in CDA systems faces many challenges, such as time-scale differences, different analysis schemes among components, cost of computation, etc. The mismatch of time scales of variability between different components, in particular, causes the coupled covariance to be dominated by noise of the variables from the fast component. Therefore, in an ensemble-based filter with a finite sample size, it is difficult to estimate the coupled covariance accurately, and sampling the coupled covariance may introduce more noise than signal and deteriorate the analysis. For instance, a recent study by Han et al. (2013) used the

biased-model framework and a simple coupled model that consists of the chaotic Lorenz-63 atmospheric equations, a two-layer ocean, and a simple sea ice model. Although their model is of similar complexity to the one in Liu et al. (2013), they found that the SCDA does not improve the analysis quality compared to the WCDA unless a very large ensemble size (10^4) is used. In addition, it is more difficult to improve the quality of analysis in the fast component through cross update, since observations from the slow component do not contain enough information about the high-frequency variability.

The physical characteristics of a coupled climate system could provide ways to improve the accuracy of sampling the cross covariance. In a typical midlatitude ocean–atmosphere coupled system, the ocean–atmosphere interaction is dominated by the stochastic forcing of the atmospheric internal variability on the slow ocean, such that the ocean–atmosphere lead–lag correlation shows a strong asymmetry. More specifically, the cross correlation is small at the zero lag and reaches maximum when the atmosphere leads the ocean by about the decorrelation time of the atmosphere (Hasselmann 1976; Barsugli and Battisti 1998). This asymmetry could potentially benefit the cross update if the high correlation between the ocean and the preceding atmosphere could be used to enhance the signal-to-noise ratio when calculating the corresponding cross covariance. To further boost the accuracy of sampling the covariance, the leading correlations could be combined with the use of time-averaged observations (Huntley and Hakim 2010), which leads to even higher correlation with the oceanic state. Some recent studies (Tardif et al. 2014, 2015) utilized the high correlations between time-averaged atmospheric and oceanic variables. In their cases without ocean observations and ODA, the slow meridional overturning circulation (MOC) benefits from the cross update using time-averaged atmospheric observations.

In this paper we will develop a new method called the leading averaged coupled covariance (LACC) method. The LACC method aims to improve the performance of the SCDA by combining the coupling dynamics with the use of time-averaged observations. Different from Huntley and Hakim (2010), the LACC method retains the higher-frequency data assimilation in the fast component. In this proof-of-concept Part I, we will test the LACC method with a simple coupled model. In Part II of this series (Lu et al. 2015, manuscript submitted to *Mon. Wea. Rev.*, hereafter Part II), we will apply the LACC method to the SCDA system in a fully coupled GCM, the Fast Ocean Atmosphere Model (Jacob
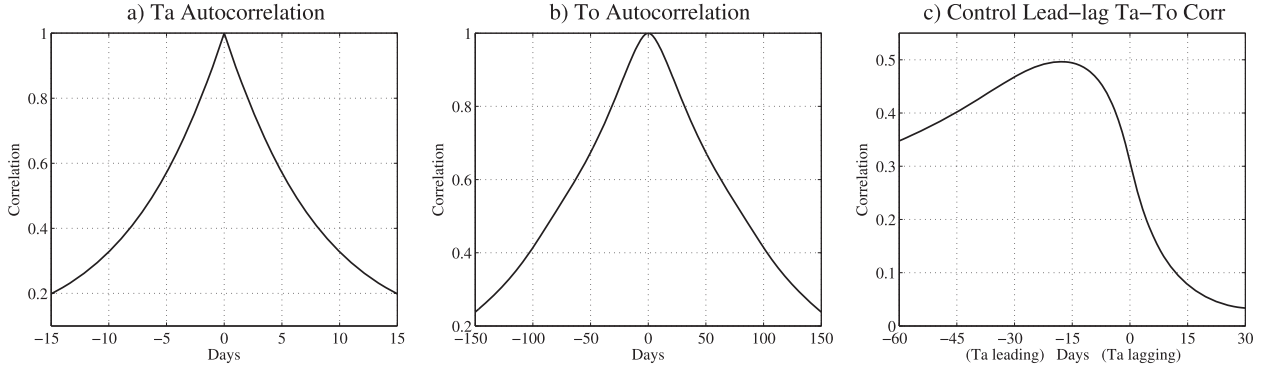
FIG. 1. (a) T_a autocorrelation, (b) T_o autocorrelation, and (c) cross correlation based on the output of a single-member control simulation.

1997). When applied to the cross update from the low-level atmosphere temperature to the sea surface temperature (SST), the LACC method significantly reduces the analysis error of monthly SST compared to the WCDA and the regular SCDA with the cross update with simultaneous coupled covariance and observation (SimCC) method.

The paper is arranged as follows. Section 2 describes our model and the LACC method, including its application to the ensemble Kalman filter (EnKF). In section 3, the performance of the SCDA with the LACC method is tested in regards to ensemble size, DA frequency, and time-scale difference. Section 4 discusses the results of different updating algorithms and schemes, as well as results within a biased-model framework. Conclusions are presented in section 5.

2. Model and methods

a. The simple coupled model

The simple model is the stochastically forced, one-dimensional, linear, coupled model of Barsugli and Battisti (1998) and Bretherton and Battisti (2000):

$$\frac{dT_a}{dt} = -aT_a + bT_o + F(t),$$

$$m\frac{dT_o}{dt} = cT_a - dT_o,$$

where T_a and T_o are the atmosphere and ocean temperature anomalies, respectively. The atmospheric component is forced by its internal variability, which is represented as the stochastic forcing of a white noise $F(t)$. The oceanic variability is driven by the atmosphere through ocean–atmosphere heat exchange. The default nondimensional parameters are $a = 1.12$, $b = 0.1$, $c = 1$, and $d = 1.08$. For illustration purposes in this study, a

shallower ($\sim$25 m) ocean mixing layer is used ($m = 10$) such that the time-scale mismatch is not too strong. The sensitivity to m will be discussed in section 3f. The autocorrelations of T_a and T_o are shown in Figs. 1a and 1b, respectively. With 1 day corresponding to a non-dimensional time of 0.1, the autocorrelation of T_a decreases to 0.5 in 7 days, while it is much longer at about 80 days for T_o. Since the slower T_o stores the cumulative effect of atmospheric forcing, the lead–lag cross correlation between T_a and T_o shows a strong asymmetry in Fig. 1c. The simultaneous correlation is only 0.3, and the correlation gradually increases as the leading time becomes longer until the peak coefficient of 0.5 is reached when T_a leads T_o by about 18 days. Since the atmospheric variability is dominated by its own random forcing, the correlation is small when the ocean leads the atmosphere (Frankignoul et al. 1998). We will only study the effect of cross update on the slow variable T_o, which is more likely to be improved by the coupled analysis (Han et al. 2013).

b. Ensemble Kalman filter with LACC

We will apply the LACC method with the sequential EnKF in this study (Houtekamer and Mitchell 2001). Hereafter, $T_a^{obs}(t)$ denotes the instantaneous atmosphere observation at time t, and has an error of σ_a. All the variables except T_a^{obs} represent their ensemble forms. Here $T_a^f(t)$ is the atmosphere forecast ensemble at time t, and $T_a^o(t)$ is the observation ensemble, generated by adding a Gaussian white noise $N(0, \sigma_a)$ onto the observation $T_a^{obs}(t)$ (Burgers et al. 1998; Houtekamer and Mitchell 1998). The terms $T_o^f(t)$ and $T_o^a(t)$ are ocean forecast and analysis ensembles, respectively. A time-averaged variable from the time τ_2 to τ_1 includes all the instantaneous states at analysis steps between τ_2 and τ_1, and is indicated by an overbar $\overline{\cdot(\tau_2, \tau_1)}$. The observation operator is not required because the observations and model states are in the same space.

In addition to the ADA and ODA, the straightforward cross update also assimilates $T_a^{\text{obs}}(t)$ to update $T_o^f(t)$ directly through the coupled covariance:

$$T_o^a(t) = T_o^f(t) + K \times [T_a^o(t) - T_a^f(t)], \quad (1a)$$

$$\text{where} \quad T_a^o(t) = T_a^{\text{obs}}(t) + N(0, \sigma_a), \quad (1b)$$

$$K = \frac{\text{cov}\langle T_o^f(t), T_a^f(t)\rangle}{\text{var}\langle T_a^f(t)\rangle + \sigma_a^2}, \quad (1c)$$

and $\text{cov}\langle \cdot, \cdot \rangle$ and $\text{var}\langle \cdot \rangle$ represent the sample covariance and sample variance, respectively. The Kalman gain K in Eq. (1c) is derived by minimizing the error variance of $T_o^a(t)$, assuming independence between the observation $[T_a^o(t)]$ and model forecast $[T_a^f(t)$ and $T_o^f(t)]$. This assumption usually holds, since the observational error originates from some external source other than the model, and the ensemble is perturbed by random Gaussian white noise. Equation (1) shows the SimCC method. The SimCC method is the straightforward way to implement cross update, and the SCDA systems of previous studies all use the SimCC method (Liu et al. 2013; Han et al. 2013). It should be remarked that even though the covariance $\text{cov}\langle T_o^f(t), T_a^f(t)\rangle$ shows up in the numerator of the Kalman gain K, the corresponding correlation determines the signal-to-noise ratio when using the sample covariance from forecast ensembles (Buehner 2005; Houtekamer et al. 2005).

Inspired by the higher cross correlation when the atmosphere leads the ocean (Fig. 1c), the atmosphere forecast $T_a^f(t)$ in Eq. (1) is replaced by the leading averaged forecast $\overline{T_a^f(\tau_2, \tau_1)}$, where τ_2 and τ_1 satisfy $\tau_2 \leq \tau_1 \leq t$. The observation $T_a^o(t)$ is also replaced by the corresponding leading averaged observation $\overline{T_a^o(\tau_2, \tau_1)}$. The analysis $T_o^a(t)$ becomes

$$T_o^a(t) = T_o^f(t) + \overline{K} \times [\overline{T_a^o(\tau_2, \tau_1)} - \overline{T_a^f(\tau_2, \tau_1)}], \quad (2a)$$

$$\text{where} \quad \overline{T_a^o(\tau_2, \tau_1)} = \overline{T_a^{\text{obs}}(\tau_2, \tau_1)} + N(0, \sigma_a/\sqrt{\tau}) \quad (2b)$$

and

$$\overline{K} = \frac{\text{cov}\langle T_o^f(t), \overline{T_a^f(\tau_2, \tau_1)}\rangle}{\text{var}\langle \overline{T_a^f(\tau_2, \tau_1)}\rangle + \sigma_a^2/\tau}. \quad (2c)$$

If a single observation $T_a^{\text{obs}}(t)$ has an error of σ_a and the errors are independent white noise, the error of the time-averaged observation $\overline{T_a^{\text{obs}}(\tau_2, \tau_1)}$ is $\sigma_a/\sqrt{\tau}$, where τ is the number of observations between τ_1 and τ_2 inclusive. Therefore, the averaged observation $T_a^o(t)$ in Eq. (2b) is perturbed by $N(0, \sigma_a/\sqrt{\tau})$, and its variance is reduced accordingly to σ_a^2/τ in Eq. (2c).

The process described by Eq. (2) varies with the choice of τ_1 and τ_2.

- $\tau_2 = \tau_1 = t$: Eq. (2) reduces to Eq. (1) and $\overline{K} = K$.
- $\tau_2 = \tau_1 < t$: A single leading atmosphere forecast $T_a^f(\tau_2)$ and the corresponding observation $T_a^{\text{obs}}(\tau_2)$ are used to update the current ocean state. According to the correlation structure in Fig. 1c, the covariance in the numerator of $\overline{K}$ could have smaller sampling error with a proper τ_2.
- $\tau_2 < \tau_1 \leq t$: Multiple leading forecasts and observations are averaged for cross update. The averaging further increases the correlation between $T_o^f(t)$ and $\overline{T_a^f(\tau_2, \tau_1)}$ and reduces the sampling error.

When $\tau_2 < \tau_1 \leq t$, Eq. (2) describes the LACC method: the cross update uses the leading averaged fast variable to calculate the coupled covariance and assimilates the corresponding leading averaged observation. More specifically, Eq. (2) will be referred to as the reperturbed LACC method due to the reperturbation of the averaged observation in Eq. (2b). Equation (2b) uses the instantaneous ocean forecast $T_o^f(t)$ instead of the averaged $\overline{T_o^f(\tau_2, \tau_1)}$ because averaging the much slower ocean does not change the cross correlation significantly. In this study, τ_1 is always set to t to include the most current observation, while τ_2 varies to change the number of averaged forecasts and observations. The reason for $\tau_1 = t$ will be discussed in section 3d.

c. Correlated observation and forecast

The change from Eq. (1) to (2) raises an important issue: the correlation between the observation and the forecast. In an SCDA system, each model component has its own data assimilation besides the cross update. For example, if $\tau_2 = \tau_1 = t - 1$ in Eq. (2), the ADA has assimilated the observation $T_a^{\text{obs}}(\tau_2)$, or more specifically the perturbed ensemble $T_a^o(\tau_2)$, to update $T_a^f(\tau_2)$ at time τ_2. When the next forecast $[T_a^f(t)$ and $T_o^f(t)]$ is generated by the coupled model, the observed information is transferred from the analyzed $T_a^a(\tau_2)$ to the ocean through dynamic coupling. Later the cross update assimilates the previous observation $T_a^{\text{obs}}(\tau_2)$, which is now correlated with both atmosphere and ocean forecasts. The correlations can be sampled from the observation ensemble $T_a^o(\tau_2)$ and the forecast ensemble $T_a^f(t)$ or $T_o^f(t)$. Similarly for the case of $\tau_2 < \tau_1 \leq t$, the time-averaged observation $\overline{T_a^o(\tau_2, \tau_1)}$ is no longer independent from either the time-averaged atmosphere forecast $\overline{T_a^f(\tau_2, \tau_1)}$ or the ocean forecast $T_o^f(t)$. This issue is not relevant with the SimCC method because all observations are new to the system when they are assimilated.

The correlation between the observation and forecast is artificially neglected in the reperturbed LACC method.

In Eq. (2), every observation $T_a^{\mathrm{obs}}(t)$, $t = \tau_2, \ldots, \tau_1$ has been independently perturbed by white noise $N(0, \sigma_a)$ to form the observation ensemble $T_a^o(t)$, $t = \tau_2, \ldots, \tau_1$ for the ADA. Later at the time of the cross update, the averaged observation $\overline{T_a^{\mathrm{obs}}}(\tau_2, \tau_1)$ is perturbed again by a new white noise $N(0, \sigma_a/\sqrt{\tau})$ that is independent from the previous perturbations used by the ADA. Even though $\overline{T_a^{\mathrm{obs}}}(\tau_2, \tau_1)$ inherits the information and errors from $T_a^{\mathrm{obs}}(t)$, $t = \tau_2, \ldots, \tau_1$, its perturbed ensemble $\widehat{T_a^o(\tau_2, \tau_1)}$ is statistically uncorrelated with the forecasts $\overline{T_a^f}(\tau_2, \tau_1)$ and $T_o^f(t)$. In other words, the implicit correlation cannot be sampled when the available observation is only a single value $\overline{T_a^{\mathrm{obs}}}(\tau_2, \tau_1)$.

Alternatively, the correlation between the observation and forecast can be explicitly estimated and included with a generalized EnKF formula. The ocean analysis is still written as

$$T_o^a(t) = T_o^f(t) + \hat{K} \times [\widehat{T_a^o(\tau_2, \tau_1)} - \overline{T_a^f}(\tau_2, \tau_1)], \qquad (3a)$$

but the new observation ensemble is the average of previously perturbed ensembles:

$$\widehat{T_a^o(\tau_2, \tau_1)} = \frac{1}{\tau} \sum_{t=\tau_1}^{\tau_2} [T_a^o(t)] = \frac{1}{\tau} \sum_{t=\tau_1}^{\tau_2} [T_a^{\mathrm{obs}}(t) + N_t(0, \sigma_a)], \qquad (3b)$$

where $N_t(0, \sigma_a)$ is the perturbation at time t, and the new Kalman gain is

$$\hat{K} = \frac{\mathrm{cov}\langle T_o^f(t), \overline{T_a^f}(\tau_2, \tau_1) - \widehat{T_a^o(\tau_2, \tau_1)}\rangle}{\mathrm{var}\langle \overline{T_a^f}(\tau_2, \tau_1) - \widehat{T_a^o(\tau_2, \tau_1)}\rangle} = \frac{\mathrm{cov}\langle T_o^f(t), \overline{T_a^f}(\tau_2, \tau_1)\rangle - \mathrm{cov}\langle T_o^f(t), \widehat{T_a^o(\tau_2, \tau_1)}\rangle}{\mathrm{var}\langle \overline{T_a^f}(\tau_2, \tau_1)\rangle - 2 \times \mathrm{cov}\langle \overline{T_a^f}(\tau_2, \tau_1), \widehat{T_a^o(\tau_2, \tau_1)}\rangle + \sigma_a^2/\tau}. \qquad (3c)$$

Here $\hat{K}$ is derived by minimizing the error variance of $T_o^a(t)$ without the assumption of independence between the observation and forecast (see appendix). Unlike Eq. (2b), Eq. (3b) requires that previous observation ensembles $T_a^o(t)$, $t = \tau_2, \ldots, \tau_1$ be stored and averaged to generate $\widehat{T_a^o(\tau_2, \tau_1)}$. By inheriting the perturbations from previous observation ensembles, $\widehat{T_a^o(\tau_2, \tau_1)}$ is explicitly correlated with the forecast ensembles $\overline{T_a^f}(\tau_2, \tau_1)$ and $T_o^f(t)$.

The method outlined by Eq. (3) will be referred to as the complete LACC method because it includes all the covariances during the derivation. The reperturbed LACC is chosen as our default method in section 3. Its performance will be compared with the WCDA and the SCDA with the SimCC method. The complete LACC method will be discussed in section 4a.

d. Cross localization

Spatial localization has been widely used to address sampling errors when small ensembles are used to sample the covariance between two separate locations (Hamill et al. 2001; Houtekamer and Mitchell 1998). When a state variable is physically located far from an observation, the error covariance tends to be small and noisy. The same problem exists for cross covariance, which is usually small and noisy because of the time-scale difference. The idea of spatial localization can also be applied between different model variables that have small and noisy correlations. For example, Kang et al. (2011) used "variable localization" to remove the

spurious correlations between uncorrelated variables. Instead of completely removing the cross covariance, which would result in the WCDA, we apply a "cross-component localization" (cross localization for short) by multiplying α (weight factor) onto the analysis increments. The ocean analysis in Eq. (2a) becomes

$$T_o^a(t) = T_o^f(t) + \alpha \times \overline{K} \times [\overline{T_a^o}(\tau_2, \tau_1) - \overline{T_a^f}(\tau_2, \tau_1)]. \qquad (4)$$

Mathematically, the cross localization works as covariance inflation and optimizes the filter performance. A smaller α indicates less adjustment to the forecast (prior) ensemble and a larger analysis (posterior) ensemble spread. The optimal weight factors are selected by trial-and-error experiments. Cross localization is not the only way to optimize the performance of cross update. For example, in Part II of this series, the more robust relax-to-prior (RTP) scheme (Zhang et al. 2004) is used and satisfactory results are achieved without much tuning of the RTP factor.

e. Cross-update frequency

Another issue related to the LACC method is the frequency of cross update. There are two approaches to this issue. As in Eq. (2), the number of averaged observations is τ.

1) Chunk scheme: The cross update is done every τ ADA cycles, and every time τ atmosphere observations are averaged. No observation is used by more than one cross update.

2) Running scheme: The cross update is done every ADA cycle, and every time previous τ atmosphere observations are averaged in a running-mean fashion.

Both schemes have some disadvantages. With the chunk scheme, the ocean states are updated less frequently if $\tau > 1$. With the running scheme, the observations are repeatedly used by the cross update. Since the error variance of the time-averaged observation is already reduced to σ_a^2/τ [denominator of Eqs. (2c) and (3c)], the information from each observation is utilized τ times in the running scheme, thus, underestimating the uncertainty of the observations. In section 3, the chunk scheme is used as default, while the two schemes are compared in section 4b.

3. Experiments and results

a. Experiment design

A perfect-model framework is used unless otherwise specified. A 101-yr integration of the model is performed starting from an initial vector of zeros, and the first year for spinning up is removed. The observations are generated at the end of each day (also the time of analysis in the experiments) by adding random Gaussian errors onto the instantaneous model states. The standard deviations of the observational errors are 0.05 for T_a and 0.02 for T_o, which are 15% and 20% of their climatological standard deviations, respectively. An ensemble size of 20, similar to previous studies (Liu et al. 2013; Han et al. 2013), is used for all experiments except section 3e.

The benchmark experiments use a WCDA system, in which observations of T_a or T_o are only allowed to update their observed variable. The assimilation is performed every day for ADA and every 5 days for ODA unless otherwise specified. The benchmark experiments with the WCDA are performed for every experiment configuration, and the results are shown as the horizontal dash–dot lines in all applicable figures. Each experiment lasts 100 years, and it usually reaches equilibrium in a couple of months because of the assimilation of high-frequency T_a observations. All statistics are computed using the final 90 years of the output. Every experiment configuration in this study is repeated 10 times with different observational errors to verify the statistical significance. The difference between different trials of the same configuration is much smaller than the mean value, usually by two orders of magnitude, so only the mean results are shown in sections 3 and 4.

To evaluate the assimilation results, we use the mean absolute error (MAE) of the ensemble mean T_o

compared to the "truth" at every ADA step. There are two important remarks about this evaluation. First, only T_o is evaluated because the one-way cross update only affects T_o, so hereafter any mention of the MAE represents the MAE of the ensemble-mean T_o compared to the truth. In a CDA system, the improved quality of ocean analysis could potentially improve the atmosphere through dynamic coupling, however, the T_a analysis is dominated by its own ADA, and all experiments have almost identical quality of atmosphere analysis. Second, the errors are calculated at every ADA step from a mix of T_o forecasts (prior) and analyses (posterior). In the SCDA system with the LACC method, T_o analyses are generated at ODA steps and cross-update steps. When the averaging length of the LACC method is different, the frequency of cross update changes and so do the steps when T_o analyses are available. To conduct a fair comparison, the ensemble mean T_o at every ADA step, no matter if it is forecast or analysis, is included for the evaluation.

b. Cross correlation from the WCDA

The cross correlation between T_a and T_o is further examined here based on the ensemble output of the WCDA system. Different from the control correlation in Fig. 1c, the ensemble correlation in Fig. 2 captures the correlation caused by the initial error growth, and is directly used by the cross update in the SCDA system.

The addition of ADA and ODA significantly transforms the lead–lag correlation structure. Figure 2a shows the mean value of the lead–lag ensemble correlation $(\mathrm{corr}\langle T_o^f(t), T_a^f(t_1)\rangle, t_1 = t - 40, t - 39, \ldots, t + 10)$. Compared to Fig. 1c, the correlations are smaller at all leads and lags, and the peak correlation occurs when T_a leads T_o by only 1 day. Because the update with perturbed observations alters the ensemble structure and reduces the ensemble spread (uncertainty) at every ADA (ODA) step, the forecast stage of every ADA (ODA) cycle starts with a different T_a (T_o) ensemble that has a relatively small spread. As a result, the largest leading correlation is limited within the first few days, and the magnitude of the correlations also differs from Fig. 1c.

The ensemble correlation between T_o and leading averaged T_a $(\mathrm{corr}\langle T_o^f(t), \overline{T_a^f}(t_2, t)\rangle, t_2 = t - 80, t - 79, \ldots, t)$ is shown in Fig. 2b. The correlation climbs rapidly at first, peaks at about 50 days, and eventually declines when the averaging length becomes longer. The correlation in Fig. 2b is directly involved in the LACC method because it determines the signal-to-noise ratio when calculating the covariance $\mathrm{cov}\langle T_o^f(t), T_a^f(\tau_2, \tau_1)\rangle$ in the numerator of Eq. (2c). Figures like Figs. 2a and 2b can be easily produced from the output of an existing
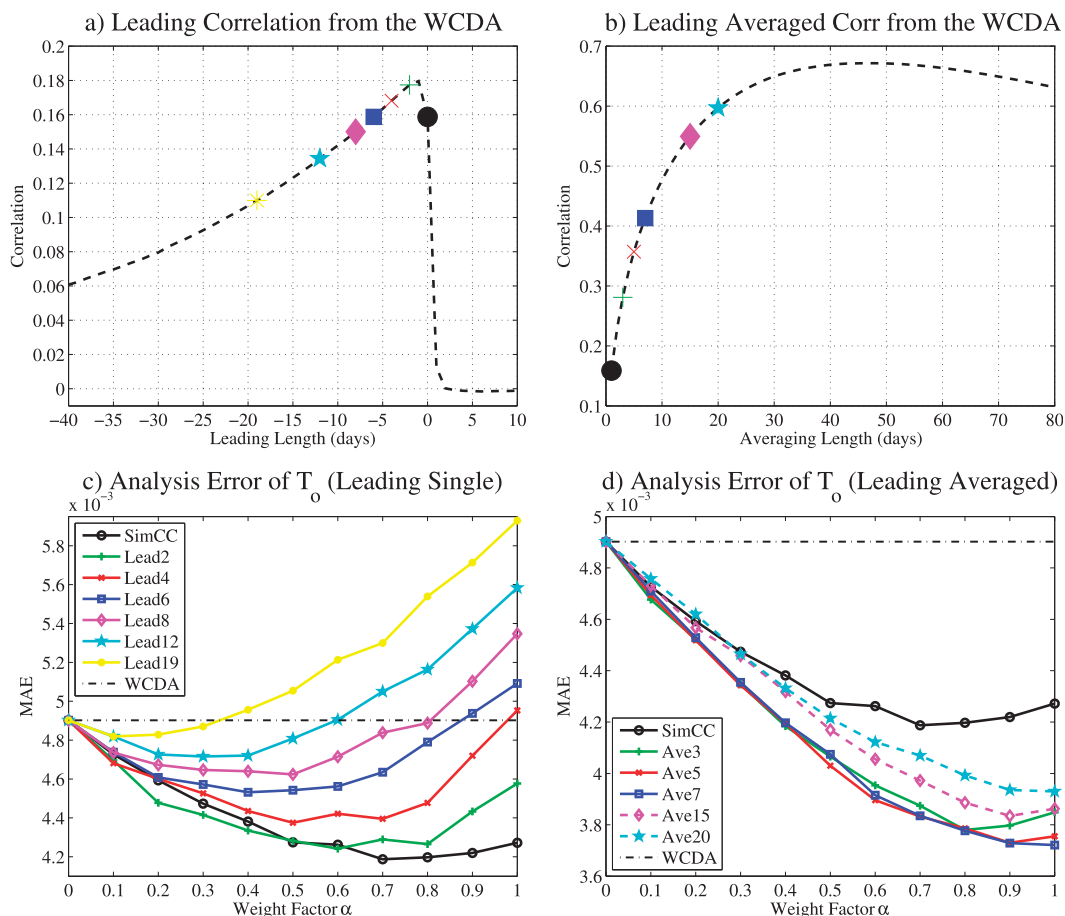
FIG. 2. (a) Lead–lag ensemble correlation and (b) leading averaged ensemble correlation based on the output of a 20-member WCDA experiment. The MAEs of SCDA experiments with (c) leading single observation and (d) leading averaged observation. The markers in (a) and (b) indicate the cross correlations used by the experiments in (c) and (d), respectively.

WCDA system and serve as a guideline to apply the LACC method to an SCDA system.

c. The SCDA experiments with the LACC method

Based on the WCDA system, cross update with the LACC method is added to set up the SCDA system. The cross update is executed independently from the ADA and ODA. Figure 2d shows the performance of the reperturbed LACC method with the chunk scheme. SimCC indicates the regular SCDA using the simultaneous coupled covariance. "Ave3" [$\tau_2 = t - 2$, $\tau_1 = t$ in Eq. (2)] uses the average of three atmosphere forecasts, including the simultaneous one and previous two. The same goes for "Ave5" and beyond. A few representative averaging lengths are selected for each graph.

In Fig. 2d, the best SimCC experiment ($\alpha = 0.7$) reduces the MAE by about 13% from the benchmark experiment (dash–dot line). This result is similar to Liu et al. (2013), but different from Han et al. (2013). The

latter found no improvement in the analysis unless the ensemble size increases to $\sim 10^4$, indicating that model biases could diminish the effectiveness of the SimCC method.

The LACC method further improves the quality of the T_o analysis. The minimal MAE, "Ave7" at $\alpha = 1$, is 11% smaller than the SimCC method and 24% smaller than the WCDA. Figure 2b shows that the leading averaged correlation increases rapidly from 0.16 for simultaneous (black dot) to 0.41 for 7 days (blue square), and larger correlations boost the signal-to-noise ratio in the calculation of the coupled covariance. According to statistics theory, the standard deviation of the sample correlation coefficient becomes smaller when sample size is larger or the "true" correlation coefficient increases (Fisher 1915).

Although the leading averaged correlation continues to rise beyond 7 days, the MAE increases when the averaging length exceeds 7 days (e.g., "Ave15" and
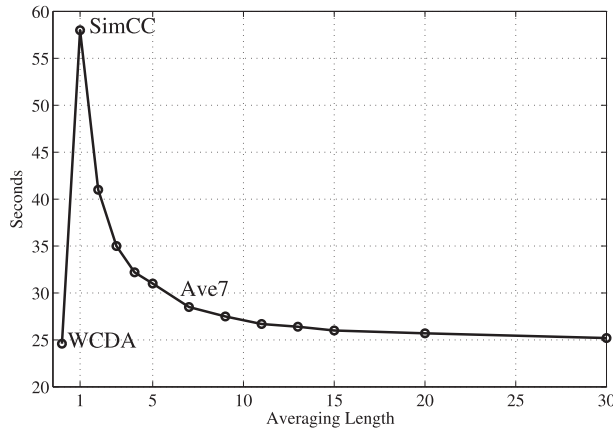
FIG. 3. Computing time of a single experiment with different methods, including the WCDA, SimCC, and LACC with different averaging lengths.

"Ave20"). For the LACC method, the optimal averaging length is primarily determined by two factors: the magnitude of the leading averaged cross correlation and the frequency of the cross update. On one hand, the correlation increases with the averaging length, for the first 50 days in this case, but the rate of increasing slows down gradually. On the other hand, a longer averaging length implies less frequent assimilation through coupled covariance and, therefore, less constraint by atmospheric observations on the ocean. When the frequency of cross update is as low as every 15 or 20 days, a majority of the T_o states are unanalyzed model forecasts, whose errors are mostly larger than analyzed model states. The competing effects of these two factors result in the optimal length of 7 days in Fig. 2d. Despite that only 30% of the T_o states are analyzed (ODA and cross update combined), the performance of Ave7 is still significantly better than the SimCC method and the WCDA, indicating the great benefits of large cross correlation and high signal-to-nose ratio using the LACC method.

The LACC method could also reduce the additional computational cost of cross update compared to the SimCC method, although the necessary sensitivity tests to tune the LACC method may offset this advantage. Figure 3 shows the computing time of a single experiment. The SimCC experiment more than doubles the computing time of the WCDA experiment, while the costs of the LACC experiments decrease in reverse proportion to the averaging length, and Ave7 only costs 15% more than the WCDA experiment.

The optimal α values also have a trend in relation to the averaging length. The minimum MAE of the SimCC method occurs when $\alpha = 0.7$, and the best

α increases to 0.8 for Ave3, 0.9 for Ave5, and finally 1.0 for Ave7, Ave15, and Ave20. In sum, the optimal α is larger when the corresponding cross correlation is higher (Fig. 2b). This relation also holds in spatial localization. Larger weights are usually prescribed for physically closer locations because of higher correlations and smaller sampling error (Mitchell and Houtekamer 2000; Hamill et al. 2001).

d. The SCDA experiments with single leading observation

As shown in Fig. 2d, the choice of averaging length is critical to the performance of the LACC method. To understand the mechanism of the LACC method better, we conduct the SCDA experiments using a single leading atmosphere forecast and observation for cross update and present the results in Fig. 2c. This set of experiments corresponds to the case of $\tau_2 = \tau_1 \leq t$ in Eq. (2). The SimCC ($\tau_2 = \tau_1 = t$) method is the same between Figs. 2c and 2d. "Lead2" ($\tau_2 = \tau_1 = t - 2$) uses the 2-day leading forecast and observation of T_a for every cross update, and the same goes for "Lead4" and beyond.

Figure 2c shows that all experiments up to "Lead19" could be better than the benchmark WCDA experiment at their optimal α values. The SimCC method produces the best analysis, which is the reason that the simultaneous observation is always included in the LACC method. The improvement from the LACC method in Fig. 2d could be seen as the combined effects of assimilating several leading observations, though it is not a simple linear combination. Considering that experiments from SimCC to "Lead6" consistently improve the analysis compared to the WCDA regardless of α, it is reasonable to expect that the optimal T_o analysis can be obtained by using atmospheric information from the simultaneous step up to 6 days before. This seems to be the case of Ave7 in Fig. 2d.

The MAE is also dependent on α in Fig. 2c. For example, the best T_o analysis is achieved with $\alpha = 0.7$ for SimCC, 0.6 for Lead2, 0.5 for Lead4, and 0.4 for Lead6. The optimal α decreases as the assimilated observation is further removed from the time of the cross update.

e. Sensitivity to ensemble size

Ensemble size is an important factor for the estimation of coupled covariance (Han et al. 2013), as well as localization and model errors (Mitchell et al. 2002). Additional LACC experiments with ensemble sizes of 10, 50, 200, and 1000 are shown in Fig. 4. Several features are noteworthy.
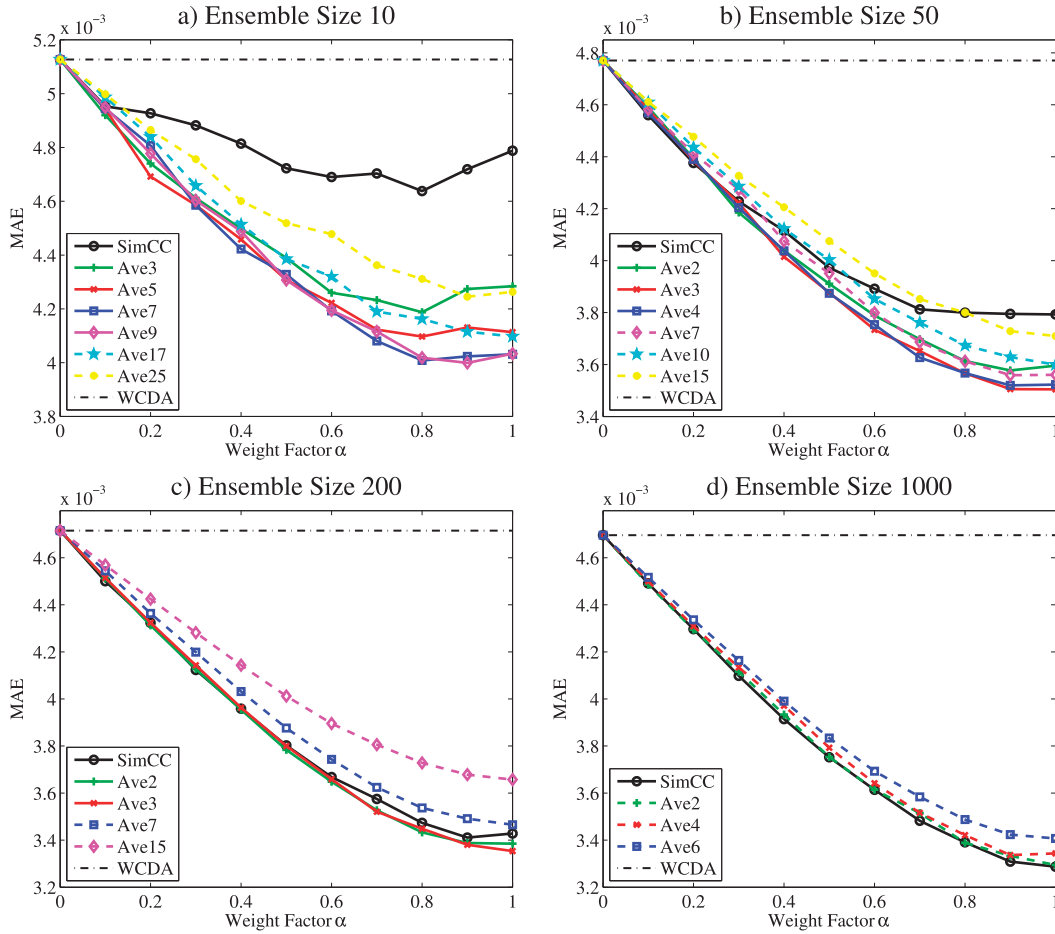
FIG. 4. As in Fig. 2d, but for ensemble sizes of (a) 10, (b) 50, (c) 200, and (d) 1000.

1) The LACC method consistently improves the SCDA compared to the WCDA, reducing the MAE by over 20% for all ensemble sizes.

2) The advantage of the LACC method over the SimCC method diminishes for larger ensembles, since larger sample sizes can reduce the sampling error of the estimated correlation (Fisher 1915) and improve the effectiveness of the straightforward cross update (Han et al. 2013). The SimCC method surpasses the LACC method when the ensemble size reaches ~10^3.

3) The optimal averaging length shortens as the ensemble size becomes larger. The experiment is Ave9 for an ensemble size of 10, Ave7 for 20, and Ave3 for 50 and 200.

4) The optimal α is mostly 1 for large ensemble sizes of 200 and 1000, showing that less covariance inflation is necessary for larger ensembles (Hamill et al. 2001).

Figure 4 shows that a sufficiently large ensemble size can significantly improve the effectiveness of the SimCC

method (e.g., Han et al. 2013), while also diminish the benefits of the LACC method. However, ensemble sizes of ~10^3–10^4 are usually not practical for state-of-the-art CGCMs. Therefore, the LACC method is an effective and efficient way to implement SCDA with moderate ensemble sizes.

f. Sensitivity to time-scale difference

The LACC method is also tested with different ocean time scales. The parameter m represents the depth of ocean mixing layer, which controls the time scale of T_o compared to T_a. Figure 5 shows the effects of different values of m on the cross correlation from single-member control simulations. A larger m of 20 increases the time scale of the ocean compared to the atmosphere, reduces the cross correlation at shorter leading times, and raises the correlation at longer leading times. A smaller m of 6 has the opposite effect.

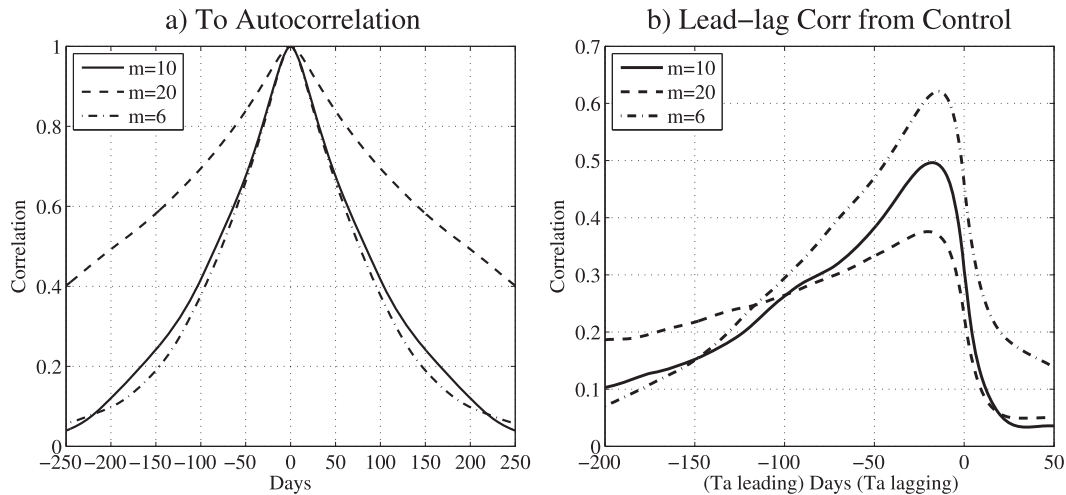The lead–lag and leading averaged ensemble correlations from WCDA experiments are also examined in

FIG. 5. As in Figs. 1b and 1c, but with additional results from the control simulations of $m = 20$ and $m = 6$.

Figs. 6a and 6b. The effect of m is similar in Figs. 6a and 5b: a larger m makes the shape of the correlation flatter. Following the change in the lead–lag correlation, the leading averaged ensemble correlation peaks at a longer averaging length and declines slower after the peak when m increases. Based on Fig. 6b, one would expect the optimal averaging length to change in the same direction as m.

Compared to the WCDA, the LACC experiments with the optimal averaging length consistently reduce the MAE by about 25% regardless of m in Figs. 6c and 6d. The optimal averaging length increases as m becomes larger (Ave3 for $m = 6$, Ave7 for $m = 10$, and Ave11 for $m = 20$), which is consistent with the trend in Fig. 6b. Physically speaking, more leading observations should be used in the case of larger m because of the longer persistence of T_o. Meanwhile, the effectiveness of the SimCC method declines as m increases and the simultaneous cross correlation decreases. The best SimCC experiments reduce the MAE by 17% when $m = 6$, 13% when $m = 10$ (Fig. 2d), and 10% when $m = 20$.

g. Sensitivity to ocean DA

Since all experiments are evaluated based on the quality of T_o analysis, it is important to assess the performance of the LACC method in relation to the quality of ODA. Experiments with daily, monthly, and zero (no ODA) ODA frequency are performed in this section. As in section 3f, the ensemble correlations based the output of the WCDA experiments are displayed in Figs. 7a and 7b. The error of the ocean observation is kept the same for all experiments. When the ODA frequency decreases, the shape of the lead–lag correlation

becomes flatter. Similar to Figs. 6a and 6b, the averaged correlation in Fig. 7b also follows the change in the lead–lag correlation.

Figures 7c–e demonstrate that the LACC method could significantly improve the analysis quality even if the ocean states are well constrained by frequent ODA. The benchmark WCDA system is increasingly better as the ODA becomes more frequent. The MAE decreases from 6.09×10^{-3} for no ODA all the way to 3.55×10^{-3} for daily ODA. Yet the improvement from the LACC method is significant for all experiments. The change in the optimal averaging length is consistent with the trend of the averaged correlation in Fig. 7b: the optimal length is shorter in the case of fast-increasing averaged correlation and longer in the case of slow-increasing correlation. Meanwhile, the advantage of the LACC method over the SimCC method becomes more substantial from Figs. 7e to 7c, showing the potential of applying the LACC method in a well-constrained WCDA system.

4. Tests on schemes and model bias

a. Complete LACC

The reperturbed LACC method is used for all experiments in section 3. Here the complete LACC method is tested with the same configuration as in Fig. 2d, and the results are reported in Fig. 8.

Figure 8 demonstrates that the complete LACC method produces almost identical results to the reperturbed LACC method (Fig. 2d). The indistinguishable results can be attributed to the strong random forcing in the model. Because of the strong forcing, every new forecast contains less persistent information from previous analysis than new information from the
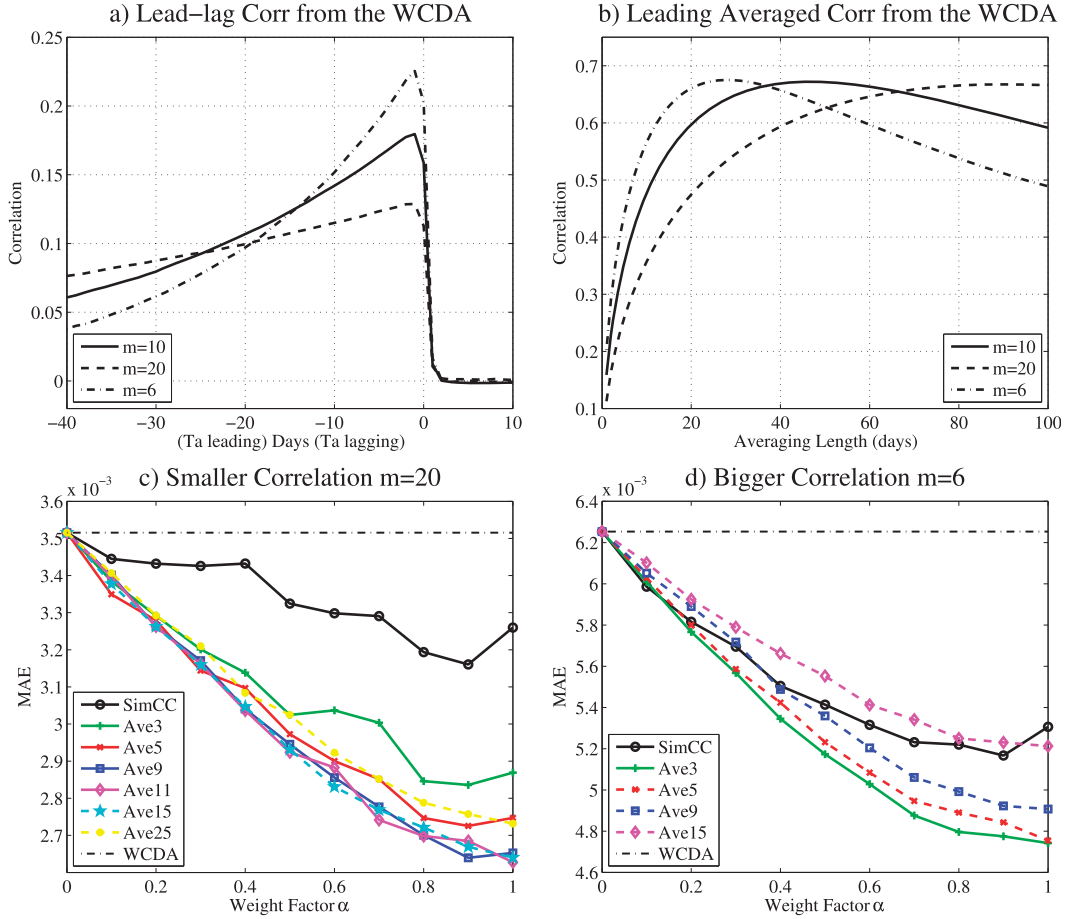
FIG. 6. (a),(b) As in Figs. 2a,b, but with additional results of (a) $m = 20$ and (b) $m = 6$. (c),(d) As in Fig. 2d, but with different model parameters (c) $m = 20$ and (d) $m = 6$.

random forcing, so those additional covariances between observations and forecasts [cov$\langle T_o^f(t), \overline{T_a^o(\tau_2, \tau_1)} \rangle$ and cov$\langle T_a^f(\tau_2, \tau_1), \overline{T_a^o(\tau_2, \tau_1)} \rangle$ in Eq. (3c)] are significantly smaller than the existing covariances in Eq. (2c), usually by one order of magnitude or more (not shown). As a result, the Kalman gain $\hat{K}$ calculated by Eq. (3c) is very close to the $\overline{K}$ by Eq. (2c).

To determine which method to use for the cross update in an SCDA system, one could estimate each term in Eq. (3c) based on the output of the WCDA system. The only modification would be saving the perturbed observation ensembles during ADA. If the covariances between observations and forecasts are significantly smaller than the other terms, namely

$$\text{cov}\langle T_o^f(t), \overline{T_a^o(\tau_2, \tau_1)} \rangle \ll \text{cov}\langle T_o^f(t), \overline{T_a^f(\tau_2, \tau_1)} \rangle \quad \text{and} \quad \text{cov}\langle \overline{T_a^f(\tau_2, \tau_1)}, \overline{T_a^o(\tau_2, \tau_1)} \rangle \ll \text{var}\langle \overline{T_a^f(\tau_2, \tau_1)} \rangle \quad \text{or} \quad \sigma_a^2/\tau,$$

the reperturbed LACC method should be acceptable. Otherwise, one should try the complete LACC method and compare the performances, since the complete LACC method could perform better because of its theoretical accuracy.

With comparable performances in this model, the reperturbed LACC method is chosen as our default because 1) the traditional EnKF formula is already used

for ADA and ODA in the WCDA system, 2) its computing time for cross update is about 10% less than the complete LACC method, and 3) no additional storage is needed for previously perturbed observation ensembles. The last reason makes it difficult to use the complete LACC method in a CGCM because saving the perturbed ensemble of every assimilated observation would require prohibitively large memory space.
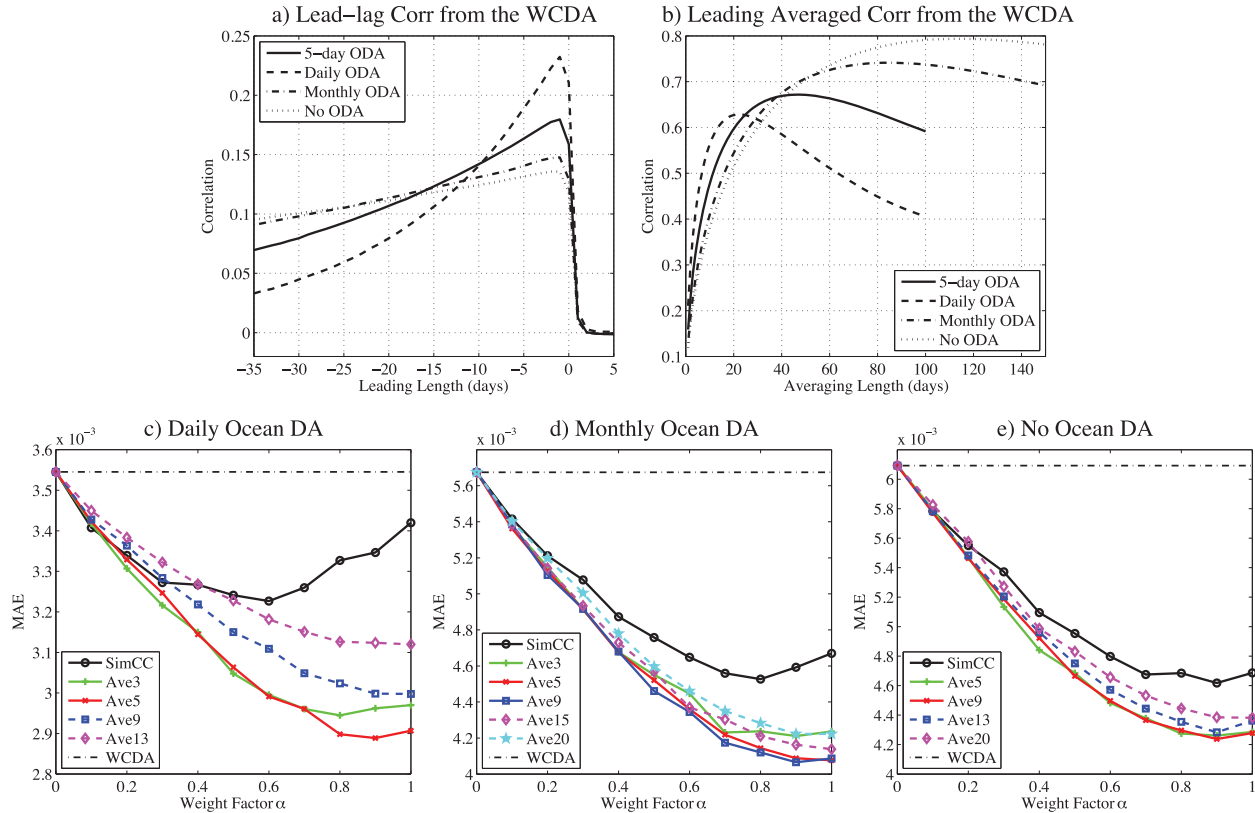
FIG. 7. (a),(b) As in Figs. 2a,b, but with additional results from WCDA experiments of daily, monthly, and no ODA. (c)–(e) As in Fig. 2d, but with different ODA frequencies of (c) daily, (d) monthly, and (e) zero (No ODA.)

b. Running scheme

All experiments so far use the chunk scheme described in section 2e. Figure 9 shows the results of the reperturbed LACC method with the running scheme, which performs the cross update at every ADA step. We also tested the complete LACC method with the running schemes and got similar results (not shown). The SimCC experiments in Fig. 9 are the same as in Fig. 2d. For Ave3, T_o is adjusted every time when T_a observation is available, and the cross update still uses the average of three leading T_a forecasts and observations like the chunk scheme, so every T_a observation is used three times. The same goes for Ave5 and beyond.

With the running scheme, the weight factor α serves the purpose of more than cross localization. As shown in Fig. 9, the best analysis of LACC experiments is achieved when α values are significantly smaller than the corresponding values with the chunk scheme (Fig. 2d). The smaller α values reduce the cross-update adjustments to counter the underestimation of observational errors, which is caused by the repeated utilization of observed information. Qualitatively, the optimal

α varies in reverse proportion to the averaging length, but other factors such as sampling errors could also affect the value of the optimal α.

In terms of analysis quality, the running scheme does perform slightly better, as the MAEs are 2%–4% smaller than the chunk scheme for most averaging lengths. This small improvement is primarily achieved by updating T_o more frequently, so that the MAE is calculated only from T_o analysis (posterior). However, the slight improvement from the running scheme requires significantly more computing time, because the running scheme costs as much as the SimCC method regardless of the averaging length.

c. Biased-model experiments

The LACC method is also tested within a biased-model framework. To set up the biased-model framework, the observations still come from the model with the default parameters, but all four parameters (a, b, c, d) in the forecast model are set 15% smaller than their default values arbitrarily. The reperturbed and complete LACC methods produce the same results, so only the reperturbed results are shown in this section.
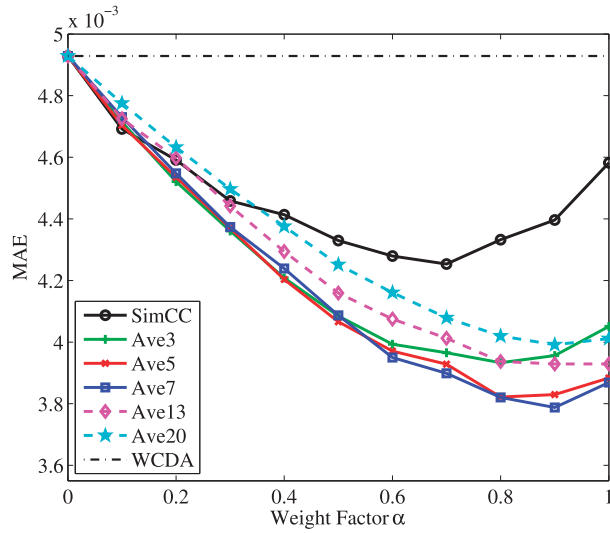
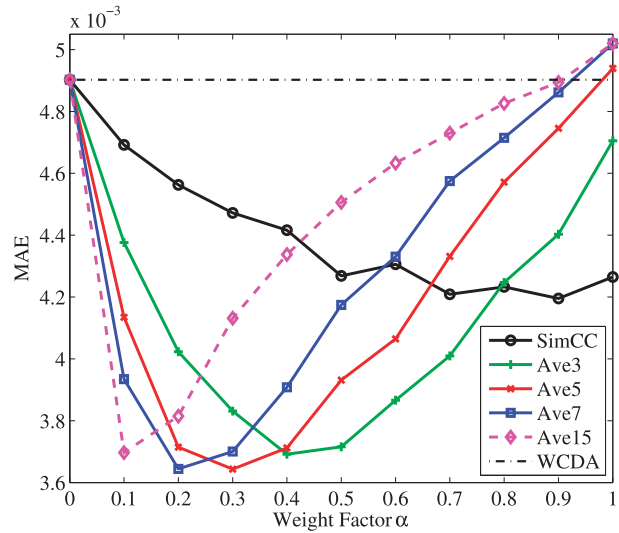FIG. 8. As in Fig. 2d, but with the complete LACC method.

FIG. 9. As in Fig. 2d, but with the running scheme for cross update.

Figure 10 shows that both the chunk and running schemes are effective with a biased model. With the presence of model biases, the MAE of the benchmark WCDA experiment increases from 4.9×10^{-3} in Fig. 2d to 8.8×10^{-3} in Fig. 10. The SimCC method performs worse than the WCDA except when $1 < \alpha < 1.6$, and the best MAE ($\alpha = 1.4$) is only 5% smaller than the WCDA. Meanwhile, the effectiveness of the LACC method is consistent. Compared to the WCDA, the chunk scheme reduces the MAE by 12% with Ave20 and $\alpha = 1$ and by 29% with Ave11 and $\alpha = 2.2$. Like in the perfect-model framework, the running scheme could outperform the chunk scheme, but only by 2%–3% for any given averaging length. The optimal α values are smaller in Fig. 10b compared to Fig. 10a, because the observations are already repeatedly used by the running scheme. Regardless of the averaging length, the best results are achieved by overweighting atmospheric observations ($\alpha > 1$). When the model parameters are biased, the analysis quality of the ocean deteriorates faster than that of the atmosphere because the higher-frequency ADA constrains the atmospheric state better. As a result, the analysis increments from the atmosphere are more accurate and should be given more confidence.

5. Summary

We have presented a new LACC method to utilize the coupled covariance in an SCDA system. By time averaging the leading model forecasts of the fast-varying variable, the LACC method significantly enhances the cross correlation between model variables with contrasting time scales and boosts the signal-to-noise

ratio when calculating the coupled covariance. The LACC method requires some modifications to the traditional ensemble-based filters, especially in regard to the additional covariances between observations and model forecasts. We have shown two ways to apply the LACC method to the EnKF—the reperturbed LACC and the complete LACC—and both produce equally improved analysis of the oceanic variable in comparison to the WCDA and the SCDA with the SimCC method.

In the simple coupled model, the SCDA system is set up by adding the cross update from the atmospheric variable to the oceanic variable. The reperturbed LACC method, along with the regular SCDA that uses the simultaneous coupled covariance, are tested with different ensemble sizes, time-scale differences, and ODA frequencies. Although the SimCC method could improve the ocean analysis compared to the WCDA, the LACC method holds a significant advantage over both the WCDA and the SimCC method. The advantage of the LACC method over the SimCC method is more notable in the cases of 1) small ensemble size, 2) larger time-scale difference, 3) small simultaneous cross correlation, and 4) more frequent ODA. In general, the LACC method suits the cases where physical correlation exists between two variables, but such correlation is too difficult to sample because of the time-scale difference.

The biased-model experiments are particularly interesting, as the SimCC method with optimal cross localization barely outperforms the WCDA. In contrast, the LACC method consistently improves the performance of the SCDA system and reduces the MAE by
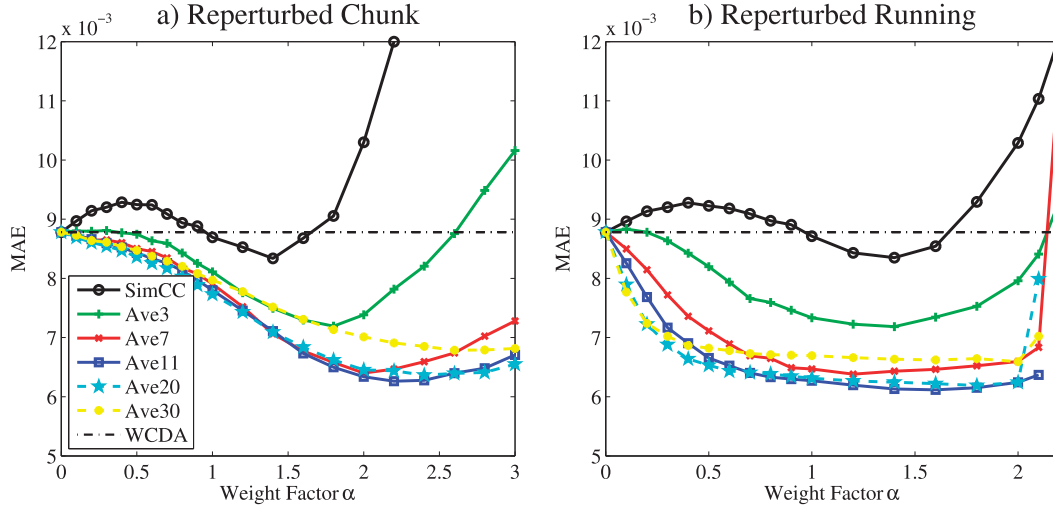
FIG. 10. As in Fig. 2d, but with (a) the chunk scheme and (b) the running scheme in a biased-model framework.

almost 30%. The effectiveness of the LACC method in the biased-model framework points to potential application in real world SCDA systems.

There are still unresolved issues with the LACC method. For example, the optimal weight factor for cross localization is determined by trial and error. The idea of adaptive inflation (Anderson 2007, 2009) could be useful to tune the weight factor and make it adaptive in time. For future research, one could continue to test the LACC method and related filtering techniques in simple conceptual models, preferably nonlinear or multidimensional like the ones used by Han et al. (2013) or Luo and Hoteit (2014).

APPENDIX

Derivation of Eq. (3)

The ocean analysis, as written in Eq. (3a), is

$$T_o^a(t) = T_o^f(t) + \tilde{K} \times [\overline{T_a^o(\tau_2, \tau_1)} - \overline{T_a^f(\tau_2, \tau_1)}]. \quad \text{(A1)}$$

Assuming the terms in Eq. (A1) are deviations from the truth, the error variance of $T_o^a(t)$ is

$$\text{var}\langle T_o^a(t)\rangle = \text{var}\langle T_o^f(t)\rangle + 2 \times \tilde{K}$$
$$\times \text{cov}\langle T_o^f(t), \overline{T_a^o(\tau_2, \tau_1)} - \overline{T_a^f(\tau_2, \tau_1)}\rangle + \tilde{K}^2$$
$$\times \text{var}\langle \overline{T_a^o(\tau_2, \tau_1)} - \overline{T_a^f(\tau_2, \tau_1)}\rangle. \quad \text{(A2)}$$

The error variance $\text{var}\langle T_o^a(t)\rangle$ can be minimized by solving

$$\frac{\partial \text{var}\langle T_o^a(t)\rangle}{\partial \tilde{K}} = 0. \quad \text{(A3)}$$

Equation (A3) gives

$$2 \times \text{cov}\langle T_o^f(t), \overline{T_a^o(\tau_2, \tau_1)} - \overline{T_a^f(\tau_2, \tau_1)}\rangle$$
$$+ 2 \times \tilde{K} \times \text{var}\langle \overline{T_a^o(\tau_2, \tau_1)} - \overline{T_a^f(\tau_2, \tau_1)}\rangle = 0. \quad \text{(A4)}$$

So the Kalman gain is

$$\hat{K} = \frac{\text{cov}\langle T_o^f(t), \overline{T_a^f(\tau_2, \tau_1)} - \overline{T_a^o(\tau_2, \tau_1)}\rangle}{\text{var}\langle \overline{T_a^f(\tau_2, \tau_1)} - \overline{T_a^o(\tau_2, \tau_1)}\rangle}. \quad \text{(A5)}$$

REFERENCES

Anderson, J. L., 2007: An adaptive covariance inflation error correction algorithm for ensemble filters. *Tellus,* **59A,** 210–224, doi:10.1111/j.1600-0870.2006.00216.x.

——, 2009: Spatially and temporally varying adaptive covariance inflation for ensemble filters. *Tellus,* **61A,** 72–83, doi:10.1111/j.1600-0870.2008.00361.x.

Barsugli, J. J., and D. S. Battisti, 1998: The basic effects of atmosphere–ocean thermal coupling on midlatitude variability. *J. Atmos. Sci.,* **55,** 477–493, doi:10.1175/1520-0469(1998)055<0477:TBEOAO>2.0.CO;2.

Bretherton, C. S., and D. S. Battisti, 2000: An interpretation of the results from atmospheric general circulation models forced by the time history of the observed sea surface temperature distribution. *Geophys. Res. Lett.,* **27,** 767–770, doi:10.1029/1999GL010910.

Buehner, M., 2005: Ensemble-derived stationary and flow-dependent background-error covariances: Evaluation in a quasi-operational NWP setting. *Quart. J. Roy. Meteor. Soc.,* **131,** 1013–1043, doi:10.1256/qj.04.15.

Burgers, G., P. J. van Leeuwen, and G. Evensen, 1998: Analysis scheme in the ensemble Kalman filter. *Mon. Wea. Rev.,* **126,** 1719–1724, doi:10.1175/1520-0493(1998)126<1719: ASITEK>2.0.CO;2.

Dee, D. P., and Coauthors, 2011: The ERA-Interim reanalysis: Configuration and performance of the data assimilation system. *Quart. J. Roy. Meteor. Soc.,* **137,** 553–597, doi:10.1002/qj.828.

Fisher, R., 1915: Frequency distribution of the values of the correlation coefficient in samples from an indefinitely large population. *Biometrika.,* **10,** 507–521, doi:10.2307/2331838.

Frankignoul, C., A. Czaja, and B. L. Heveder, 1998: Air–sea feedback in the North Atlantic and surface boundary conditions for ocean models. *J. Climate,* **11,** 2310–2324, doi:10.1175/1520-0442(1998)011<2310:ASFITN>2.0.CO;2.

Hamill, T. M., J. S. Whitaker, and C. Snyder, 2001: Distance-dependent filtering of background error covariance estimates in an ensemble Kalman filter. *Mon. Wea. Rev.,* **129,** 2776–2790, doi:10.1175/1520-0493(2001)129<2776:DDFOBE>2.0.CO;2.

Han, G. J., X. R. Wu, S. Q. Zhang, Z. Liu, and W. Li, 2013: Error covariance estimation for coupled data assimilation using a Lorenz atmosphere and a simple pycnocline ocean model. *J. Climate,* **26,** 10 218–10 231, doi:10.1175/JCLI-D-13-00236.1.

Hasselmann, K., 1976: Stochastic climate models. Part I. Theory. *Tellus,* **28A,** 473–485, doi:10.1111/j.2153-3490.1976.tb00696.x.

Houtekamer, P. L., and H. L. Mitchell, 1998: Data assimilation using an ensemble Kalman filter technique. *Mon. Wea. Rev.,* **126,** 796–811, doi:10.1175/1520-0493(1998)126<0796: DAUAEK>2.0.CO;2.

——, and ——, 2001: A sequential ensemble Kalman filter for atmospheric data assimilation. *Mon. Wea. Rev.,* **129,** 123–137, doi:10.1175/1520-0493(2001)129<0123:ASEKFF>2.0.CO;2.

——, ——, G. Pellerin, M. Buehner, M. Charron, L. Spacek, and M. Hansen, 2005: Atmospheric data assimilation with an ensemble Kalman filter: Results with real observations. *Mon. Wea. Rev.,* **133,** 604–620, doi:10.1175/MWR-2864.1.

Huntley, H. S., and G. J. Hakim, 2010: Assimilation of time-averaged observations in a quasi-geostrophic atmospheric jet model. *Climate Dyn.,* **35,** 995–1009, doi:10.1007/s00382-009-0714-5.

Jacob, R., 1997: Low frequency variability in a simulated atmosphere ocean system. Ph.D. thesis, University of Wisconsin–Madison, 159 pp.

Kang, J.-S., E. Kalnay, J. Liu, I. Fung, T. Miyoshi, and K. Ide, 2011: "Variable localization" in an ensemble Kalman filter: Application to the carbon cycle data assimilation. *J. Geophys. Res.,* **116,** D09110, doi:10.1029/2010JD014673.

Liu, Z., S. Wu, S. Q. Zhang, Y. Liu, and X. Y. Rong, 2013: Ensemble data assimilation in a simple coupled climate model: The role of ocean-atmosphere interaction. *Adv. Atmos. Sci.,* **30,** 1235–1248, doi:10.1007/s00376-013-2268-z.

Luo, X., and I. Hoteit, 2014: Ensemble Kalman filtering with a divided state-space strategy for coupled data assimilation problems. *Mon. Wea. Rev.,* **142,** 4542–4558, doi:10.1175/MWR-D-13-00402.1.

Mitchell, H. L., and P. L. Houtekamer, 2000: An adaptive ensemble Kalman filter. *Mon. Wea. Rev.,* **128,** 416–433, doi:10.1175/1520-0493(2000)128<0416:AAEKF>2.0.CO;2.

——, ——, and G. Pellerin, 2002: Ensemble size, balance, and model-error representation in an ensemble Kalman filter. *Mon. Wea. Rev.,* **130,** 2791–2808, doi:10.1175/1520-0493(2002)130<2791:ESBAME>2.0.CO;2.

Saha, S., and Coauthors, 2010: The NCEP Climate Forecast System Reanalysis. *Bull. Amer. Meteor. Soc.,* **91,** 1015–1057, doi:10.1175/2010BAMS3001.1.

Singleton, T., 2011: Data assimilation experiments with a simple coupled ocean-atmosphere model. Ph.D. thesis, University of Maryland, College Park, 116 pp.

Sugiura, N., T. Awaji, S. Masuda, T. Mochizuki, T. Toyoda, T. Miyama, H. Igarashi, and Y. Ishikawa, 2008: Development of a four-dimensional variational coupled data assimilation system for enhanced analysis and prediction of seasonal to interannual climate variations. *J. Geophys. Res.,* **113,** C10017, doi:10.1029/2008JC004741.

Tardif, R., G. J. Hakim, and C. Snyder, 2014: Coupled atmosphere–ocean data assimilation experiments with a low-order climate model. *Climate Dyn.,* **43,** 1631–1643, doi:10.1007/s00382-013-1989-0.

——, ——, and ——, 2015: Coupled atmosphere–ocean data assimilation experiments with a low-order model and CMIP5 model data. *Climate Dyn.,* doi:10.1007/s00382-014-2390-3, in press.

Zhang, F. Q., C. Snyder, and J. Z. Sun, 2004: Impacts of initial estimate and observation availability on convective-scale data assimilation with an ensemble Kalman filter. *Mon. Wea. Rev.,* **132,** 1238–1253, doi:10.1175/1520-0493(2004)132<1238: IOIEAO>2.0.CO;2.

Zhang, S. Q., M. J. Harrison, A. Rosati, and A. Wittenberg, 2007: System design and evaluation of coupled ensemble data assimilation for global oceanic climate studies. *Mon. Wea. Rev.,* **135,** 3541–3564, doi:10.1175/MWR3466.1.